IOP Publishing Nanotechnology
Nanotechnology 28 (2017) 355502 (9pp) https://doi.org/10.1088/1361-6528/aa7baa

Real time polymer nanocomposites-based physical nanosensors: theory and modeling

Stefano Bellucci[1,5], Yuri Shunin[2,3], Victor Gopeyenko[3], Tamara Lobanova-Shunina[4], Nataly Burlutskaya[3] and Yuri Zhukovskii[2]

[1] INFN-Laboratori Nazionali di Frascati, Via Enrico Fermi 40, I-00044, Frascati-Rome, Italy
[2] Institute of Solid State Physics, University of Latvia, Kengaraga Str. 8, LV-1063 Riga, Latvia
[3] ISMA University, 1 Lomonosova Str., Bld 6, LV-1019, Riga, Latvia
[4] Riga Technical University, Faculty of Mechanical Engineering, Transport and Aeronautics, 1 Lomonosova Str., Bld V, LV-1019, Riga, Latvia

E-mail: Stefano.Bellucci@lnf.infn.it, yu_shunin@inbox.lv, yuri.zhukovskii@gmail.com, viktors.gopejenko@isma.lv, natalja.burlucka@isma.lv and busus@inbox.lv

Received 22 March 2017, revised 8 June 2017
Accepted for publication 26 June 2017
Published 26 July 2017

Abstract

Functionalized carbon nanotubes and graphene nanoribbons nanostructures, serving as the basis for the creation of physical pressure and temperature nanosensors, are considered as tools for ecological monitoring and medical applications. Fragments of nanocarbon inclusions with different morphologies, presenting a disordered system, are regarded as models for nanocomposite materials based on carbon nanocluster suspension in dielectric polymer environments (e.g., epoxy resins). We have formulated the approach of conductivity calculations for carbon-based polymer nanocomposites using the effective media cluster approach, disordered systems theory and conductivity mechanisms analysis, and obtained the calibration dependences. Providing a proper description of electric responses in nanosensoring systems, we demonstrate the implementation of advanced simulation models suitable for real time control nanosystems. We also consider the prospects and prototypes of the proposed physical nanosensor models providing the comparisons with experimental calibration dependences.

Keywords: real time nanosensors, functionalized nanocomposites, physical nanosensors

(Some figures may appear in colour only in the online journal)

1. Introduction

We focus our research on two important directions of real-time control nanosystems addressed to ecological monitoring and medical applications, both of which provide environmental security for human society and every individual. Ecological monitoring has been widely presented in [1]. For individual application, it is necessary to develop nanodevices with various functions for the human body, particularly, for the control of health parameters, the enhancement of human abilities, and prosthetics. Another course of development of nanosensors, nanoactuators, nanotransducers, etc—is the creation of artificial systems such as artificial intelligence or artificial individual [2, 3].

Nanosensor systems constitute an essential functional part of any modern device that provides information processing for information systems, engineering interfaces, healthcare and many others. The talk is about nanosensor systems for various aspects of ecological monitoring and security. The fundamental electronic devices are nanocarbon-based field-effect transistors (FET) capable of providing high sensitivity to various external influences of different nature. In particular, changes of local electronic density of states correlate with corresponding physical, chemical and bio-chemical influences and lead to FET-device conductivity changes [3]. Conventional schemes of nanosensoring systems are based on nano-FET-type devices [1, 3, 4]:

(a) general nanocarbon-based FET-type devices: unperturbed FET based on carbon nanotube (CNT)- or graphene nanoribbon (GNR)-based FETs are mainly

[5] Author to whom any correspondence should be addressed.

composed of the corresponding semiconducting carbon materials suspended over two electrodes;

(b) physical nanosensors: a conducting threshold can be altered when the tube or graphene ribbon is bent;

(c) chemical nanosensors: the same threshold can be altered when the amount of free charges on the tube of graphene ribbon surface is increased or decreased by the presence of donor or acceptor molecules of specific gases or composites;

(d) biological nanosensors: ensure monitoring of biomolecular processes such as antibody/antigen interactions, DNA interactions, enzymatic interactions or cellular communication processes, etc.

However, these types of nanosensors are oriented on local external influences at atomic or molecular levels, when the external agent has a direct contact with nanocarbon surface atoms, like in FET-type nanosensors.

The current research is devoted to the modeling of nanocarbon polymer nanocomposite-based physical nanosensors intended for pressure and temperature. The sensitivity of the considered nanosensors in this case depends on percolation ability of a nanocomposite subdued to the changes of physical factors (pressure or temperature). Attention should be paid to the nanoscaled quantum mechanical phenomenon of percolation ability among the neighboring nanocarbon 'islands' within a nanocomposite. Integrated 'micro' or 'meso'-scale conductivity effects should also be evaluated as a goal for calibration of a nanocomposite material as a measurement tool for pressure or temperature.

2. Methods and models

We consider physical nanosensors (pressure and temperature) based on functionalized CNTs and GNRs nanostructures. The model of nanocomposite materials based on carbon nanocluster suspension (CNTs and GNRs) in dielectric polymer environments (e.g., epoxy resins) is regarded as a disordered system of fragments of nanocarbon inclusions with different morphologies (chirality and geometry) in relation to a high electrical conductivity in a continuous dielectric environment. The electrical conductivity of a nanocomposite material depends on the concentration of nanocarbon inclusions (in fact, carbon macromolecules) and corresponding morphologies. We should evaluate the role of particular local conductivity mechanisms in nanocomposites using the cluster approach based on the multiple scattering theory formalism, realistic analytical and coherent potentials, as well as effective medium approximation (EMA) which we have effectively used for modeling of nanosized systems, especially for various nanointerconnects problems [5, 6]. We have found during conductivity calculations in CNT-metal and GNR-metal interconnects that the conductivity mechanism is very sensitive to local morphological disordering [7–9].

2.1. Conductivity mechanisms

Considering models of physical nanosensors using CNTs- and GNRs-based nanocomposites, we should discuss conductivity mechanisms. In particular, in a medium with practically essential conductivity, it is useful to consider the phenomenon through the contributions of scattering effects that can take place in nanocomposite materials. We focus our attention on the four possible ways (see figure 1) trying to find the best description, in particular, for functionalized nanocomposites.

The key parameter for the analysis is the mean scattering length $\ell_{\text{e-gen}}$ of an electron in the conductive matter. In general, $\ell_{\text{e-gen}}$ includes various contributions in accordance with the well-known Matthiessen's rule, stating:

$$\frac{1}{\ell_{\text{e-gen}}} = \frac{1}{\ell_{\text{e}-\text{e}}} + \frac{1}{\ell_{\text{e-a/phon}}} + \frac{1}{\ell_{\text{e-o/phon}}} + \frac{1}{\ell_{\text{e-o/phot}}} + \frac{1}{\ell_{\text{e-impurity}}} + \frac{1}{\ell_{\text{e-defect}}} + \frac{1}{l_{\text{e-boundary}}} + \ldots, \quad (1)$$

where $\ell_{\text{e}-\text{e}}$ is the electron–electron scattering length, $\ell_{\text{e-a/phon}}$ is the acoustic phonon (emission and absorption) scattering length, $\ell_{\text{e-o/phon}}$ is the optical phonon emission scattering length, is the optical phonon absorption scattering length, is the electron-impurity scattering length, $\ell_{\text{e-o/phot}}$ is the electron-defect scattering length, $\ell_{\text{e-impurity}}$ is the electron scattering length with the boundary.

Hydrodynamical character of electric conductivity is the fundamental property of certain metals at low temperatures [10, 11]. This quality can be observed for such cases, when the length of electron mean free path is the order of the sample character size, namely, $\ell_{\text{e-boundary}} \propto L$ and $l_{\text{e}-\text{e}} \ll L$.

The last relation should be specified in cases of collisional and non-collisional electronic plasma with concentrations less than $10^{17}\,\text{cm}^{-3}$. Hydrodynamical behavior of electron liquid can be observed in some critical spaces of metal-like graphene-based electronic devices [12].

Collisional mechanism is a more expanded conductivity mechanism and takes place in most cases of typical normal conditions, e.g., for metals and semiconductors. In this case $\ell_{\text{e-phon}} \propto a \ll L$, where a is the character distance between 'scatterers'—atoms. This mechanism for DC-conductivity is described by the classical Drude model [13, 14]: $\sigma = \frac{ne^2\tau_{\text{e-a/phon}}}{m^*}$, where n is the electron concentration, e is the electron charge, $\tau_{\text{e-phon}}$ is the time electron-phonon scattering, m^* is the effective mass of electron.

Ballistic character of conductivity is characterized by transport of electrons in a medium having negligible electrical resistivity caused by scattering. Moreover, the scattering character is essentially elastic and the medium should be considered ideally regular. The time of electron–phonon interaction is negligible. This mechanism is observed, for example, in GNRs and CNTs included in FET-type devices. The most popular description of ballistic mechanism was given by Rolf Landauer and is known now as Landauer–Büttiker formalism [15]. Landauer formula $G(\mu) = G_0 \sum_n T_n(\mu)$, where G is the

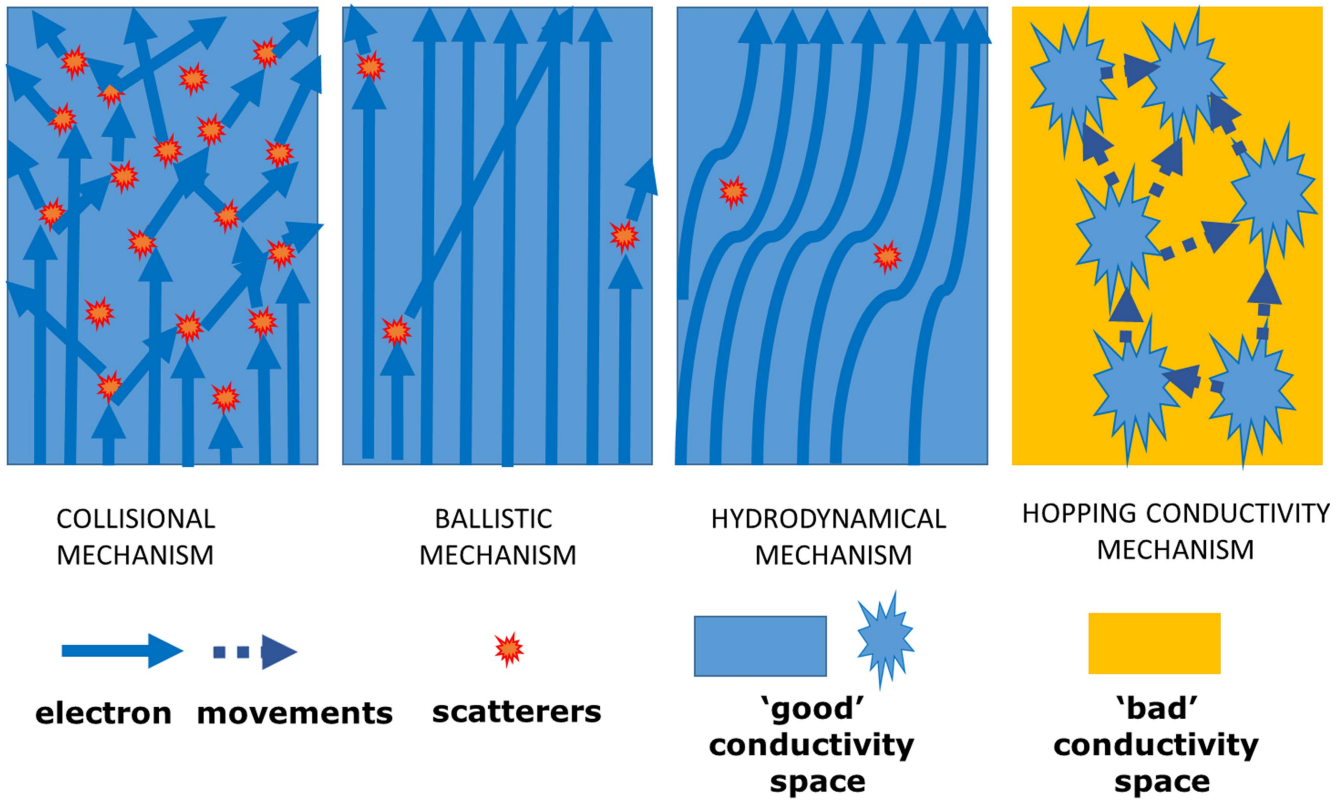

Figure 1. Review of general mechanisms of electron DC-conductivity.

electrical conductance, $G_0 = e^2/(\pi\hbar) \approx 7.75 \times 10^{-5}$ Ohm is the conductance quantum, $T_n(\mu)$ is the transmission eigenvalues of the channels, and the sum runs over all transport channels in the conductor. The conductance can be calculated as the sum of all the transmission possibilities that an electron has when propagating with an energy E equal to the chemical potential μ. In fact, the phenomenon is similar to optical thin films effect, when the transparency is achieved due to the quantization of the wave length. However, it is impossible to realize the remarkable conductivity property of GNRs and CNTs without any contacts. Appropriate nanocarbon-metal interconnects are characterized as disordered regions with essentially scattering mechanism of conductivity.

Hopping conductivity mechanism was proposed for disordered condensed systems (e.g., for composite amorphous semiconductors and dielectrics) for the explanation of the metal–insulator transition [16]. The talk is about the existence of the electron hopping between the conductive clusters in the dielectric, or between the impurity centers of localization. In this model, the medium (insulator–metal) is represented by the following pattern: there is a random distribution of the nodal points related to each other by 'conductivities' exponentially dependent on the interstitial distances. The hopping conductivity model with a variable 'jump' length can be considered the most general one $\ell_{\text{e-impurity}} \propto a$:

$$\sigma = \sigma_0 \exp\left(-\frac{4}{3}\left(\frac{4\alpha r_s}{a}\right)^{3/4}\left(\frac{W}{\kappa T}\right)^{1/4}\right), \qquad (2)$$

where a is the characteristic 'borous radius' of the considered 'doping' center, r_s is the characteristic radius of the doping center or conductive region, W is the characteristic potential barrier for electron tunneling, k is the Boltzmann constant, T is the sample temperature, $\alpha \approx 0.70$ is the empirical constant which can be evaluated only using Monte-Carlo numerical simulations [17], σ_0 is the pre-exponential factor is calculated taking into account the character of localization centers distribution.

2.2. Models CNTs- and GNRs-based nanocomposites

We develop a set of prospective models of nanocarbon-based nanomaterials and nanodevices having various interconnects and interfaces. In particular, nanoporous and nanocomposite systems are considered as complicated ensembles of basic nanocarbon interconnected elements (e.g., CNTs or GNRs with possible defects and dangling boundary bonds) within the effective media type environment. Interconnects are essentially local quantum objects and are evaluated in the framework of the developed cluster approach based on the multiple scattering theory formalism as well as EMA [3, 7, 18].

In cases when nanocarbon clusters are embedded in high resistance media (instead of vacuum) we come to a nanocomposite material. The utilization of polymeric composite materials (e.g., epoxy resins) supplemented with various morphological nanocarbon groups of CNTs and GNRs allows us to create effective pressure and temperature sensors. Application of such nanocomposites as coatings can provide

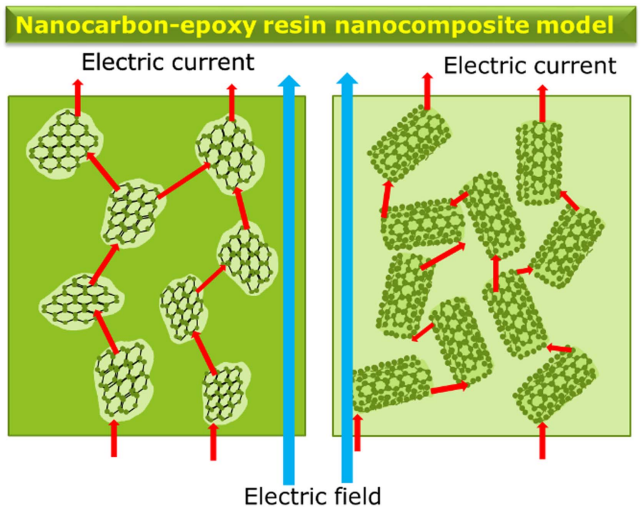

Figure 2. Model of composite polymer material with carbon nanocluster inclusions of GMRs- and CNTs-types.

continuous monitoring of the mechanical strains in piping systems (for example, in aircraft or automotive applications), when the critical pressure values can indicate malfunctions of the engine. The analysis of possible medical instruments for real-time measuring human body temperature and blood pressure can also be realized.

The interest in CNTs and GNRs-based polymer nanocomposites as prospective pressure and temperature nanosensor materials is based on the observed electric percolation phenomena via the nanocarbon inclusions concentration. In particular, the electrical conductivity of a nanocomposite increases with the increasing CNT loading up to a critical filler concentration, where a dramatic increase in conductivity is observed. This critical filler concentration is called electrical percolation threshold concentration. At percolation threshold concentration, a filler forms a three-dimensional conductive network within the matrix, hence electron can tunnel from one filler to another and, in doing so, it overcomes the high resistance offered by insulating polymer matrix.

Consider the model of composite material with carbon nanocluster inclusions of CNTs- and GNRs-types (see figure 2).

The host material—is a flexible dielectric medium of epoxy resin-type with high resistance [19]. However, a low concentration of nanocarbon inclusions cannot change the mechanical properties of the host material. At the same time, high electrical conductivity of CNTs- and GNRs incorporated in the host material can significantly affect the total conductivity of the nanocomposite material. According to our model, the mechanism of these changes is related to the effects of percolation through the hopping conductivity (see figure 3). This is the only mechanism that takes into account the compliance with our analysis induced morphological changes in the whole nanocomposite matrix. This is a single mechanism which takes into account accordance with our

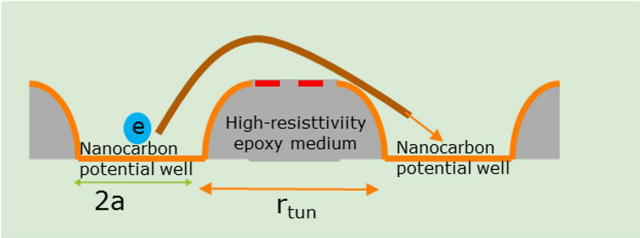

Figure 3. Potential wells model for hopping in polymer nanocomposistes, where $2a$ is the characteristic size of nanocarbon inclusion, r_{tun} is the length of the tunnel 'jump' of the electron.

analysis induced morphological changes in the whole nanocomposite matrix.

Thus, the model of nanocomposite materials based on carbon nanocluster suspension (CNTs and GNRs) in dielectric polymer environments (e.g., epoxy resins) is considered as a disordered system of fragments of nanocarbon inclusions with different morphology (chirality and geometry) in relation to a high electrical conductivity in a continuous dielectric environment. Presumably, the electrical conductivity of a nanocomposite material will depend on the concentration of nanocarbon inclusions (in fact, carbon macromolecules). Isolated nanocarbon inclusions will provide conductivity due to the hopping conductivity mechanism through dangling bonds up to the percolation threshold, when at high concentrations (some mass %) a sustainable ballistic regime appears, which is characteristic of pure carbon systems. The hopping mechanism is regulated by the electron hopping between 'nanocarbon macromolecules' (see, (1) and [3, 16, 18]:

$$\sigma = \sigma_0 \exp\left(-\frac{4}{3}\left(\frac{4\alpha r_{tun}}{a}\right)^{3/4}\left(\frac{W_0}{\kappa T}\right)^{1/4}\right), \qquad (3)$$

where r_{tun} is the length of the tunnel 'jump' of the electron equal to the distance between 'nanocarbon' clusters, σ_0 is the pre-exponential normalization factor, which means the conductivity of monolithic dielectric medium. This factor can be evaluated following the relationship:

$\sigma_0 = \frac{16e^2 r_{tun}^3 N}{\pi\hbar a_0}$, where N is the concentration of localization centers, in our case, nanocarbon inclusions concentration. For arbitrary distribution of localization centers $r_{tun}^3 N = 0.24$ [22].

Added to this is the effect of intrinsic nanocarbon cluster conductivity, which is dependent on its morphology. The electric conductivity will also depend on the spatial orientation of nanocarbon inclusions. It will be greater for the longitudinal electric field orientations and lower for the transverse ones. Of course, any spatial orientations are technologically possible. If we introduce the volume part as an indicator of the nanocarbon inclusions concentration: $\eta = \left(\frac{R_0}{R_0 + r_{tun}}\right)^3$, where is the average nanocarbon macromolecule radius, R_0 is, as earlier, the statistically averaged width of the potential barrier between the nearest nanoclusters, which is responsible for percolation ability of the model nanocomposite. We should also diminish the hopping

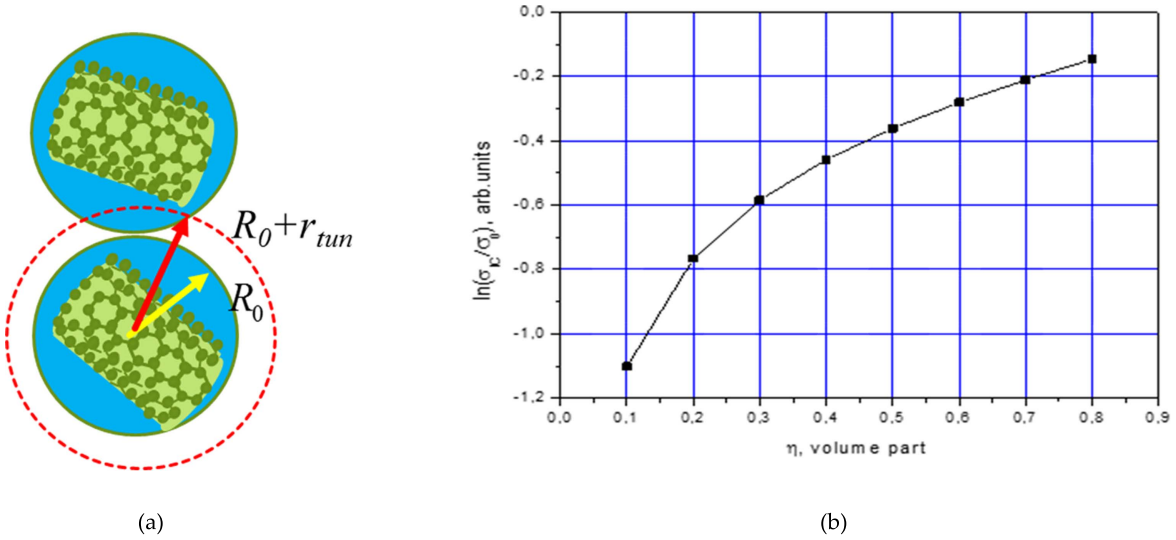

(a) (b)

Figure 4. Typical statistically averaged morphology of CNT-polymer nanocomposite: (a) structural model; (b) the hopping conductivity correlation via the average nanocarbon macromolecules volume part within continuous dielectric medium.

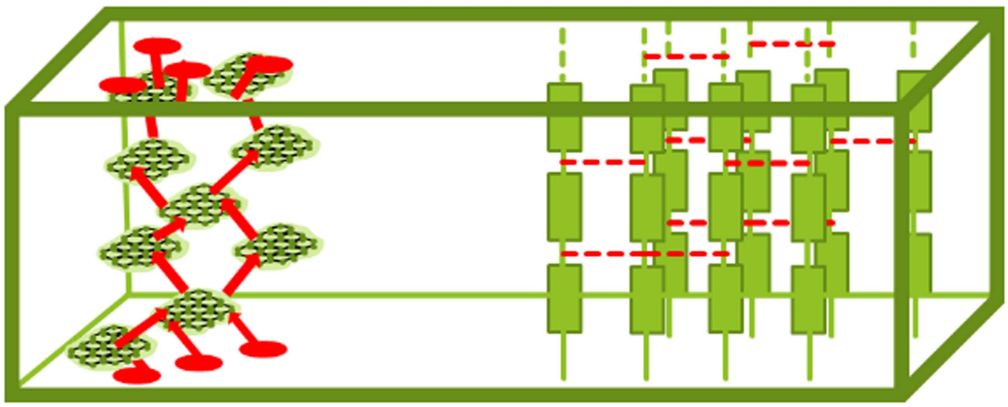

Figure 5. Principle equivalent scheme of nanocomposite model for resistance calculation.

phenomena and percolation probability taking into account the nanocarbon macromolecule orientation within a hypothetical sphere embedded into high resistance dielectric medium. Based on this definition, we can obtain a contribution of potential nanocarbon clusters to nanocomposite conductivity as follows (see also figure 4):

$$\ln\left(\frac{\sigma}{\sigma_0}\right) = -\frac{4}{3}\left(\frac{4\alpha}{3}R_0(\eta^{-1/3}-1)\right)^{3/4}\left(\frac{W_0}{\kappa T}\right)^{1/4}. \quad (4)$$

The overall conductance of nanocomposite material is evaluated using equivalent electric scheme (see figure 5 and [19]):

$$\Sigma \approx \Sigma_D + \Sigma_{NC},\ \Sigma_{NC} = \sum_{i=1}^{N}(R_i)^{-1},$$
$$R_i = A\sum_{k=1}^{N_i}\left(\sigma_{\text{nano},ik}^{-1} + \sum_{k=0}^{N_i}(N_{\text{eff},ik\sigma}\sigma_{\text{jump},ik})^{-1}\right), \quad (5)$$

where N—is the number of conductivity channels, N_i– is the number of nanocarbon clusters in the conductivity channel, N_{eff} is the number of effective tunneling bonds including the contact region, $\Sigma_D = (R_D)^{-1}$ is the conductance of dielectric medium, σ_{nano} is the conductivity nanocluster, σ_{jump}—is the hopping conductivity of the effective bond, which creates interconnect for large nanocarbon inclusion concentrations.

Basic nanocomposite models for simulation are presented in figure 6.

3. Simulation of stress- and temperature-induced resistance of carbon-based nanocomposite sensors: results and discussions

The basic dimensions of nanocarbon clusters (CNTs and GNRs) are as follows: the diameter of the CNT—5 nm, the height—10 nm, the width of the expanded CNT, i.e., the width of the GNR $= \pi \cdot 5 \approx 15.6$ nm. The total height of model sensor is accepted as 100 nm.

The average statistical distance between nanocarbon clusters is −5 nm. This is the key distance for the mechanism of hopping conductivity. Nanocarbon cluster is considered as a potential well with a typical size $2a$. Neighboring potential wells are separated by a distance r_{tun}. These two parameters are ultimately determine the morphology of the nanocomposite material. For modeling it also necessary to recalculate a

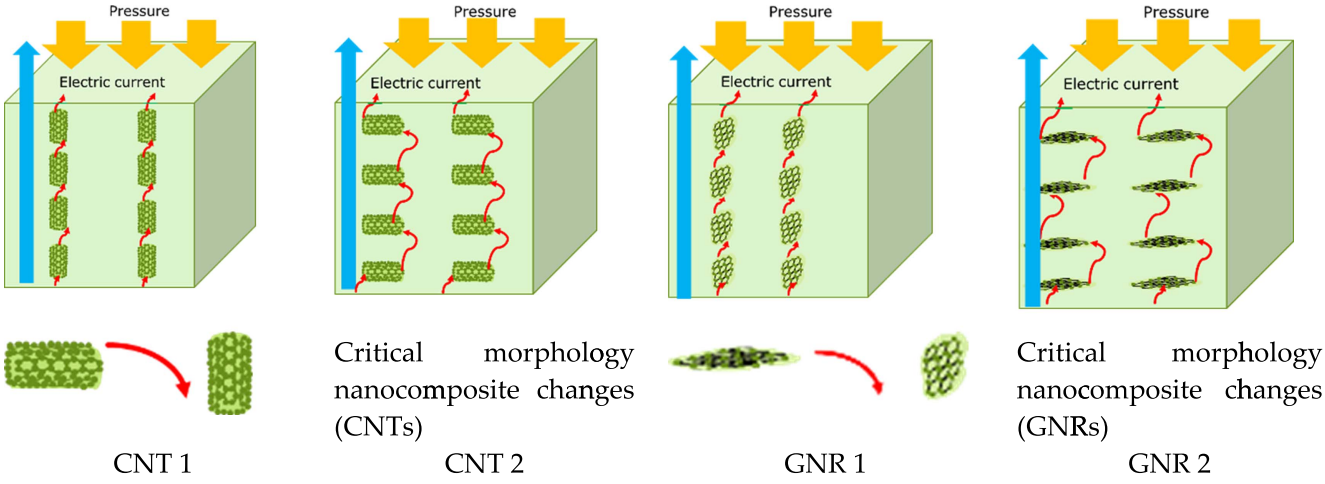

Figure 6. Models of nanocarbon-based functionalized polymer nanocomposites: CNT configuration 1, CNT configuration 2, GNR configuration 1, GNR configuration 2, ↑- electric field direction.

microscopical parameter of relativive jumpimg length to macroscopic strain parameter $\varepsilon = \Delta L/L$ in Hook's law $\sigma = E\varepsilon$, where L is the total sample length. In cases of longitudinal orientation of CNTs (configuration CNT 1) the recalculation looks as: $\varepsilon = \frac{\Delta L}{L} \approx \frac{\Delta r}{r} \cdot \frac{1}{1 + \frac{1}{1+(1/n)} \cdot \frac{l}{r}}$, where l is the CNT length (close to $2a$) and n is the number of CNT inclusions along the line (current direction). For transversal CNTs orientations (configuration CNT 2) the similar recalculation looks as: $\varepsilon = \frac{\Delta L}{L} \approx \frac{\Delta r}{r} \cdot \frac{1}{1 + \frac{1}{1+(1/n)} \cdot \frac{d}{r}}$, where d is the diameter of the CNT.

In cases of longitudinal orientation of GNRs (configuration GNR 1) the recalculation looks as : $\varepsilon = \frac{\Delta L}{L} \approx \frac{\Delta r}{r} \cdot \frac{1}{1 + \frac{1}{1+(1/n)} \cdot \frac{h}{r}}$, where h is the GNR height (close to $2a$) and n is the number of GNR inclusions along the line (current direction).

For transversal GNRs orientations (configuration GNR 2) the similar recalculation looks as: $\varepsilon = \frac{\Delta L}{L} \approx \frac{\Delta r}{r}$, where d is the diameter of the GNR.

The proposed model of hopping conductivity for current percolation in carbon-based epoxy-resin nanocomposite takes into account basically the percolations along the nanocluster sets which are located along the stress direction. Interactions between the neighboring sets are not considered for a low general concentration of nanocarbon inclusions.

Figure 7 demonstrates resistance correlations via static stresses for ideal morphologies of a nanocomposite when CNTs and GNRs are oriented pure longitudinally, pure transversely. Configurations CNT 2(min) and CNT 4(max) correspond to the minimal and maximal tunneling (jumping) distances due to the angle deviation of CNTs relatively longitudinal orientation.

From the technological point of view, it is not so simple to provide such ideal orientations for host polymer materials similar to epoxy resins. The first problem of the nanocomposite morphology is the selection of CNTs and GNRs with identical parameters. The second problem is the polymer-nanocarbon mixture creation when we evidently should expect a homogenous random distribution of nanocarbon orientations.

Figure 8 demonstrates the marginal rotational disordering of CNTs inclusions from 'ideal' longtitudinal orientation. Deviations of orientations give the characterictic intercluster distances of 3.82 (see figure 7(a), Configurations 2, 3) and 7.02 nm (see figure 7(a), Configurations 4) taking into account basic 5 nm in the ideal case.

Figures 7 and 8 present the full-scale simulation of CNTs orientation deviations within a host material. The results show various sensitivity of the model nanocomposite as a potential pressure nanosensor in dependence of its morphology. Configurations of the 4th type (see, figure 6) are more sensitive and, evidently, more practically preferable.

The model uses morphologically compatible carbon nanoconfigurations with the same number of carbon atoms, the same surface area of model CNTs and GNRs, and the same chirality. In this way, the model CNTs and GNRs are interconnected by a simple topological transformation from a cylinder to a rectangular fragment.

3.1. Modeling and experimental results

In this section, we will discuss the correlation of simulation results for pressure and temperature nanosensors with the experimental data of the particular prototype of similar devices [20], where the developed technology of functionalized nanocomposite based on epoxy resin (*ED*-20, *GOST* 10587-84. *Epoxy-Diane Resins Uncured, elasticity modulus* $E = 3.05$ GPa, *mass density* $\rho_m = 1.16$–1.25 g cm^{-3}) with multi-wall CNTs inclusions was applied. The testing of the mentioned nanosensors with various CNTs morphologies (longitudinal and transverse) and mass concentrations (1%, 2%, 3%) was carried out.

When testing the pressure sensor, the load ranged from 0 to 500 N, which corresponds to the change in pressure from 0 to 30 Bars. The pressure test was carried out on a machine

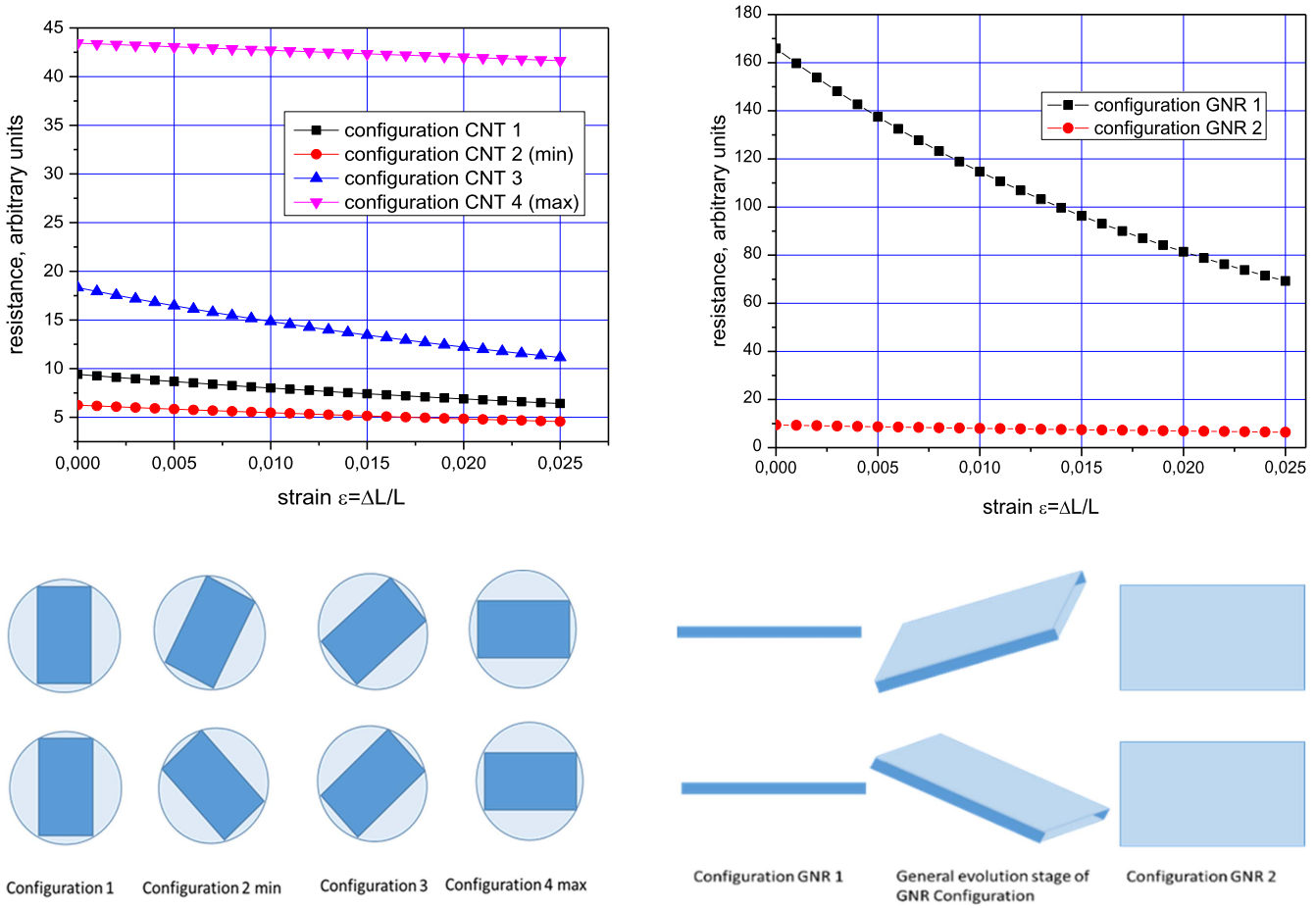

Figure 7. Simulation of nanocarbon composites resistances via strain: (a) CNTs configurations, (b) GNRs configurations.

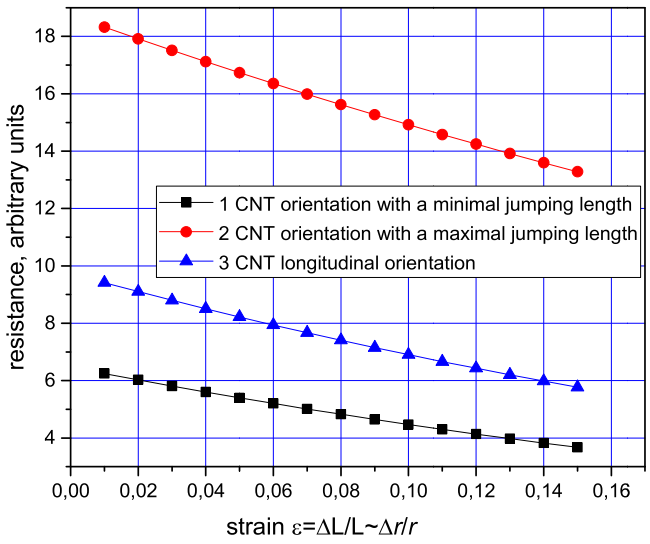

Figure 8. Simulation of nanocarbon composites resistances via strain for rotational deviations of CNTs inclusions.

Instron 5942. The typical dependence of the sensor resistance on the pressure changes, as compared with the simulation results, is shown in figure 9(a). Small deviations are connected with technological problems in the reproduction of perfect morphology, which reduces the percolation limit of the nanocomposite.

The typical dependence of the temperature sensor in the temperature range of 27 °C–90 °C compared with the simulation results is shown in figure 9(b). The temperature test was carried out using a Brookfield TC-502 water bath. The sensor sample was protected with a waterproof bag and placed in a water bath. The discrepancy in behavior between the experimental and theoretical dependencies is associated with morphological imperfections of the real sensor induced the orientation dispersion of CNTs. This effect can diminish the hopping mechanism efficiency, especially, for the higher temperatures.

Modeling of resistivity dependence via weight fraction of CNTs is presented in figure 10, where the sharp changes of resistivity within the weight fraction interval (0.08–0.12) is

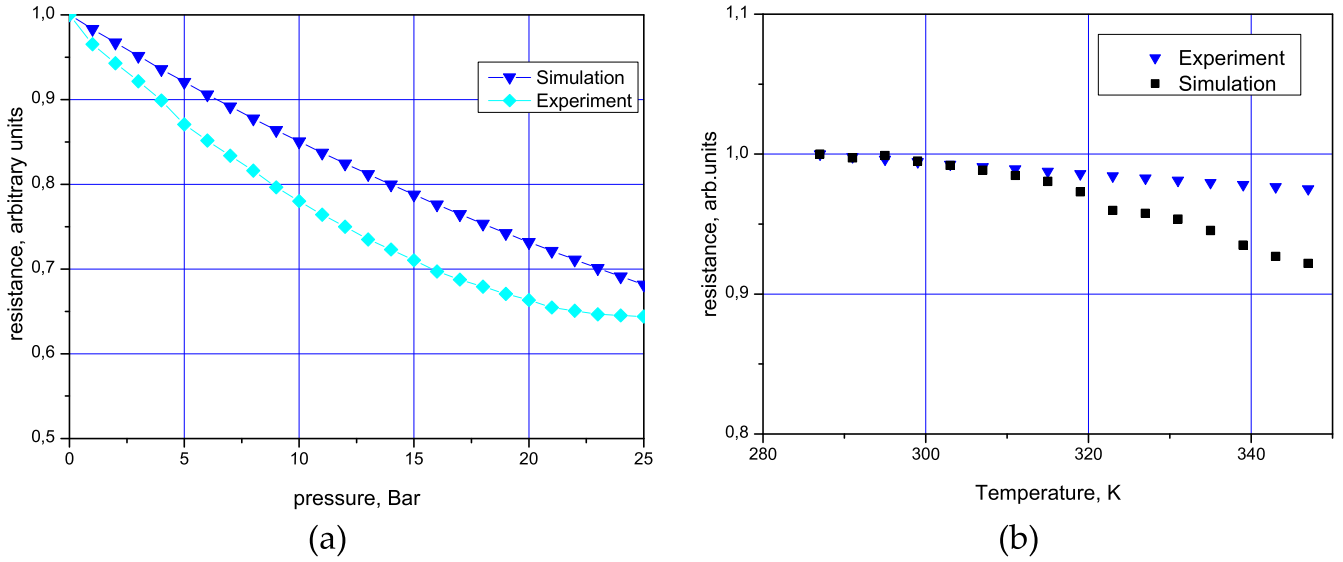

Figure 9. Comparison of real pressure and temperature nanosensor indications [20] with more adequate models morphologies simulation: (a) pressure nanosensor; (b) temperature nanosensor.

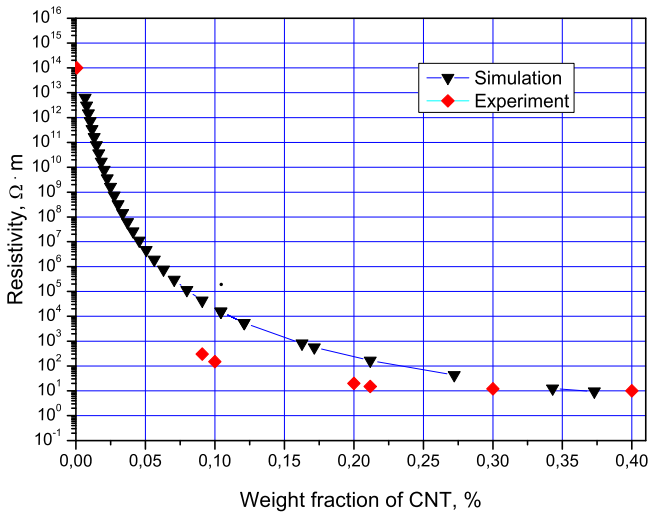

Figure 10. Comparison of resistivity of developed model CNT-based nanocomposite via weight fraction of CNT with the experimental data [21].

observed. Evidently, this phenomenon can be explained by the increase in the percolation processes under the growing CNTs weight fraction.

4. Conclusions

The prototypes of nanocomposite pressure and temperature nanosensors have been simulated. The hopping conductivity mechanism gives the adequate description of possible nanosensor qualities. An important problem in manufacturing sensors based on CNTs and GRNs is nanocarbon inclusions orientation, which determines the electrical properties of the future nanosensors. Various nanocomposite morphologies are considered and computer simulation results for pressure and temperature nanosensor models are presented in comparison with the experimental nanodevice prototype. A good correlation between the proposed nanocomposite-based sensor model and the experimental one was shown. The developed mathematical model can be applied to polymer nanocomposites with inclusions of different type. Various morphologies of resistive network models can be realized for evaluation of the total resistance in different nanosensor prototypes.

Acknowledgments

This research has been partially supported by Belarus-Latvia Bilateral Project ‘Correlation of electromagnetic, mechanical and heat properties of aerogels and polymer composites with nanocarbon inclusions’ (2014–2015), grant ‘Nanostructures for bacteria detection and study’ (NANOBAC) (01.10.2015–31.12.2017) Ministry of Education and Science of the Republic of Kazakhstan (2015–2017) and Ventspils Higher School Research Division.

Author Contributions

Evaluating the contribution of the research team members we should point out that V I Gopeyenko and N Yu Burlutskaya made a large amount of calculations, Yu F Zhukovskii made the critical analysis of CNTs and GNRs applications, Yu N Shunin, T Lobanova-Shunina, and St Bellucci made the review of theoretical approaches and wrote most of the manuscript.

Conflicts of interest

‘The authors declare no conflict of interest.’

References

[1] Shunin Y and Kiv A (ed) 2012 *Nanodevices and Nanomaterials for Ecological Security* (*Series: NATO Science for Peace Series B—Physics and Biophysics*) (Heidelberg: Springer) 363p

[2] Shunin Y N, Zhukovskii Y F, Gopeyenko V I, Burlutskaya N Y and Bellucci S 2012 Properties of CNT- and GNR-metal interconnects for development of new nanosensor systems *Nanodevices and Nanomaterials for Ecological Security* (*Series: NATO Science for Peace Series B—Physics and Biophysics*) ed Y Shunin and A Kiv (Heidelberg: Springer) pp 237–62

[3] Shunin Y, Bellucci S, Zhukovskii Y, Lobanova-Shunina T, Burlutskaya N and Gopeyenko V 2015 Modelling and simulation of CNTs- and GNRs-based nanocomposites for nanosensor devices *Comput. Modelling New Technol.* **19** 14–20

[4] Shunin Y N, Gopeyenko V I, Burlutskaya N, Lobanova-Shunina T and Bellucci S 2013 Electromagnetic properties of CNTs and GNRs based nanostructures for nanosensor systems *Proc. Int. Conf., Physics, Chemistry and Application of Nanostructures-Nanomeeting—2013 (Minsk, Belarus)* ed V E Borisenko *et al* (New-Jersey, London, Singapore: World Scientific) pp 250–3

[5] Shunin Y N and Schwartz K K 1997 Correlation between electronic structure and atomic configurations in disordered solids *Computer Modelling of Electronic and Atomic Processes in Solids* ed R C Tennyson and A E Kiv (Dodrecht/Boston/London: Kluwer Acad. Publisher) pp 241–57

[6] Shunin Y N and Shvarts K K 1986 Calculation of the electronic structure in disordered semiconductors *Phys. Status Solidi* b **135** 15–36

[7] Shunin Y N, Zhukovskii Y F, Gopeyenko V I, Burlutskaya N, Lobanova-Shunina T and Bellucci S 2012 Simulation of electromagnetic properties in carbon nanotubes and graphene-based nanostructures *J. Nanophotonics* **6** 061706

[8] Shunin Y N, Zhukovskii Y F, Gopejenko V I, Burlutskaya N and Bellucci S 2011 *Ab initio* simulations on electric properties for junctions between carbon nanotubes and metal electrodes *Nanosci. Nanotechnol. Lett.* **3** 816–25

[9] Shunin Y N, Zhukovskii Y F, Burlutskaya N and Bellucci S 2011 Resistance simulations for junctions of SW and MW carbon nanotubes with various metal substrates *Cent. Eur. J. Phys.* **9** 519–29

[10] Landau L D 1957 The theory of a fermi liquid *Sov. Phys.-JETP* **3** 920–5
Landau L D 1956 *Exp. Theor. Phys.* **30** 1058–64

[11] Gurzhi R P and Shevchenko S I 1968 Hydrodynamic mechanism of electric conductivity of metals in a magnetic field *Sov. Phys.-JETP* **27** 1019–22

[12] Mendoza M, Herrmann H J and Succi S 2013 Hydrodynamic model for conductivity in graphene *Sci. Rep.* **3** 1052

[13] Drude P 1900 Zur Elektronentheorie der metalle *Ann. Phys., Lpz.* **306** 566

[14] Drude P 1900 Zur Elektronentheorie der Metalle: II. Teil. Galvanomagnetische und thermomagnetische Effecte *Ann. Phys., Lpz.* **308** 369

[15] Landauer R 1957 Spatial variation of currents and fields due to localized scatterers in metallic conduction *IBM J. Res. Dev.* **1** 223–31

[16] Mott N F 1968 Metal–insulator transition *Rev. Mod. Phys.* **40** 677–83

[17] Seager C H and Pike G E 1974 Percolation and conductivity: a computer study: II. *Phys. Rev.* B **10** 1435–46

[18] Shunin Y N, Gopeyenko V I, Burlutskaya N Y, Lobanova-Shunina T D and Bellucci S 2015 Electromechanical properties of carbon-based nanocomposites for pressure and temperature nanosensors *EuroNanoForum* **2015** 1–12 http://euronanoforum2015.eu/wp-content/uploads/2015/03/Abstract_Shunin.pdf

[19] Shunin Y, Bellucci S, Zhukovskii Y, Gopeyenko V, Burlutskaya N and Lobanova-Shunina T 2015 Nanocarbon electromagnetics in CNT-, GNR- and aerogel-based nanodevices: models and simulations *Comput. Modelling New Technol.* **19** 35–42

[20] Abdrakhimov R R, Sapozhnikov S B and Sinitsin V V 2013 Pressure and temperature sensors basis of ordered structures of carbon nanotubes in an epoxy resin *Bull. South Ural State Univ. Ser. Comput. Technol., Autom. Control, Radio Electron.* **13** 16–23

[21] Zhou Y X, Wu P X, Cheng Z-Y, Ingram J and Jeelani S 2008 Improvement in electrical, thermal and mechanical properties of epoxy by filling carbon nanotube *Express Polym. Lett.* **2** 40–8

[22] Shklovski B I and Efros A L 1979 *Electronic Properties of Doped Semiconductor* (Moscow: Nauka) (in Russian)
Shklovski B I and Efros A L 1984 *Electronic Properties of Doped Semiconductors* (Heidelberg: Springer)